Extraction of Rare Earth Elements from Organic Acid Leachate Using Formo-Phenolic-like Resins

Evan Lelong, Julien Couturier, Clément Levard, Stéphane Pellet-Rostaing, Guilhem Arrachart

recycling

MDPI

Article

Extraction of Rare Earth Elements from Organic Acid Leachate Using Formo-Phenolic-like Resins

Evan Lelong [1], Julien Couturier [2,3], Clément Levard [2], Stéphane Pellet-Rostaing [1] and Guilhem Arrachart [1,*]

[1] ICSM, Univ Montpellier, CEA, CNRS, ENSCM, 30207 Marcoule, France
[2] Aix-Marseille Univ, CNRS, IRD, INRAE, CEREGE, 13545 Aix-en-Provence, France; levard@cerege.fr (C.L.)
[3] European Synchrotron Radiation Facility (ESRF), 38000 Grenoble, France
* Correspondence: guilhem.arrachart@umontpellier.fr; Tel.: +33-4-66-79-15-68

Abstract

Formo-phenolic-like resins were synthesized by replacing phenol with phloroglucinol, a biobased and biocompatible compound, and using different aldehydes, such as biomass-derived furaldehyde and glyoxal. Studies on the adsorption of rare earth elements from an aqueous organic acid solution indicate that these resins follow the Langmuir isotherm model, with maximum adsorption capacities ranging from 0.38 to 0.75 mmol/g. Adsorption was temperature-independent but strongly influenced by pH, with an up to fourfold increase between pH 2 and 5. Extraction kinetics were rapid, reaching equilibrium within two hours. Complete metal recovery was achieved within ten minutes using a 1 mol/L HCl desorption solution. Selectivity also varied with pH; glyoxal- and furfural-based resins showed superior separation performance at pH 2–3 and 3–4, respectively. The application of this method to real-world samples, including permanent magnet and red mud organic acid leachates, demonstrated effective extraction of rare earth elements and promising selectivity over iron (Fe), cobalt (Co), and nickel (Ni).

Keywords: rare earth elements; organic acid leachate; formo-phenolic resins; sorbents

Academic Editors: Ana Paula Paiva and Akira Otsuki

Received: 23 June 2025
Revised: 24 July 2025
Accepted: 11 August 2025
Published: 17 August 2025

Citation: Lelong, E.; Couturier, J.; Levard, C.; Pellet-Rostaing, S.; Arrachart, G. Extraction of Rare Earth Elements from Organic Acid Leachate Using Formo-Phenolic-like Resins. *Recycling* **2025**, *10*, 165. https://doi.org/10.3390/recycling10040165

1. Introduction

Rare earth elements (REEs)—fifteen lanthanides, scandium, and yttrium—are currently classified as critical materials due to the steady growth in their consumption because of new technologies [1,2]. The extraction process of REEs from mines is dominated by a few countries, and their cost and environmental impact will continue to increase. The pursuit of new sources of REEs has become increasingly critical in addressing supply chain vulnerabilities and reinforcing strategic resource independence [3,4]. While considerable research has focused on recycling REE-rich materials such as urban mine waste and end-of-life permanent magnets, other promising avenues remain underexplored. Notably, certain types of mining byproducts—such as bauxite residue—have been shown to contain significant concentrations of REEs, reaching up to 2700 mg/kg [5]. These underutilized materials represent a viable secondary resource for REE recovery and warrant further investigation as part of a diversified supply strategy [6–8].

Among hydrometallurgical processes, strong acidic leaching (HNO_3, H_2SO_4, HCl) followed by liquid–liquid extraction is considered the reference process for REE extraction from mines and waste [9]. However, the use of strong acids and large volumes of organic solvents raise health and environmental concerns.

The leaching of REEs from ores or waste materials using organic acids has emerged as an environmentally friendly alternative to traditional inorganic acid leaching [10,11]. Indeed, some organic acids can be produced from biomass, and solid adsorbents can be reused to avoid the problems associated with organic solvents, such as volatility, third-phase formation, and decomposition.

The leaching of REEs from NdFeB magnets has been demonstrated to be an efficient process when using organic acids (acetic, citric and tartaric acids, for example), minimizing the leaching of iron and other matrix components [12–14]. In the context of bauxite residue (red mud), organic acids like citric or lactic acid can effectively solubilize REEs through chelation and acid dissolution mechanisms [15,16]. Other secondary sources, including phosphate residues [17], coal fly ash [18], and electronic waste [19–21] also show promising REE leaching behavior with organic acids, offering selective recovery with reduced environmental impact.

Furthermore, solid-phase extraction is easier to implement than liquid–liquid processes. Various organic materials have been reported in the literature for the solid–liquid extraction of REEs [22], including polymers [23–25], phenolic polymers [26–31], modified silica [32–34], carbon particles [35–37], and impregnated resins [38–40]. The main challenges in developing organic adsorbents are combining high adsorption capacity with fast kinetics, ensuring good selectivity towards the targeted elements, preventing aggregation during the process, enabling the easy back-extraction of metals, and ensuring reusability.

Therefore, an interesting approach to recovering REEs involves leaching with organic acids followed by solid–liquid extraction. This appears to be an effective and suitable method [41,42].

With this in mind, the present study investigated the preparation of formo-phenolic-like resins for the extraction of REEs from organic acid leachate. In this process, phenol was substituted with phloroglucinol, a less toxic [43] and more biocompatible compound noted for its antispasmodic properties and high reactivity in polymerization reactions. Moreover, this triol is currently synthesized using a chemical process, but it could be produced using a greener process [44]. To discuss the effect of the aldehyde on the extraction properties, four aldehydes were used: formaldehyde, furfural, glyoxal, and terephthalaldehyde. The selection of these aldehydes was made with the intention of modulating the spacing between phloroglucinol units and the level of crosslinking [44–46]. Furthermore, furfural and glyoxal can be produced from renewable biomass resources, such as biobased xylose or ethylene glycol, respectively [45,46]. After a thorough study of the adsorption properties in acetic acid, the prepared materials were employed for metal extraction from the leachate of permanent magnets in acetic acid at a concentration of 1.6 mol/L as well as bauxite residue in acetic, citric, or lactic acid.

2. Results and Discussion

2.1. Resin Synthesis and Characterizations

The resins were obtained using a standard polymerization process with alkaline catalysis by means of sodium hydroxide [31]. Phenol, which is commonly used and classified as CMR 2, was substituted with **Ph**loroglucinol (Figure 1). This triol was pre-polymerized using **F**ormaldehyde (3 eq), **Fu**rfural (2 eq), **Gly**oxal (1 eq), or terephthalaldehyde (**TPA**, 1 eq) in a water/ethanol mixture (1/1) and then cured at 130 °C for 48 h. The four resulting insoluble materials, Ph-F, Ph-Fu, Ph-Gly, and Ph-TPA, were used for characterization and extraction tests. Solid-state ^{13}C NMR, FT-IR, and TGA analyses were performed and are presented in the Supplementary Materials (Figures S1–S3). Examination of the crushed resins by SEM showed that their morphology is typical of unmodified bulk formo-phenolic resins (Figure S4). The material appears as a densely packed structure composed of particles

with a rough surface texture. The absence of any visible pore openings or interconnected porous network indicates that the sample likely has a low surface area and minimal inherent porosity. An analysis of the data has indicated no significant disparities in terms of morphology when comparing the various sorbents. This observation suggests that the nature of the aldehyde does not appear to exert any influence on the observed outcomes.

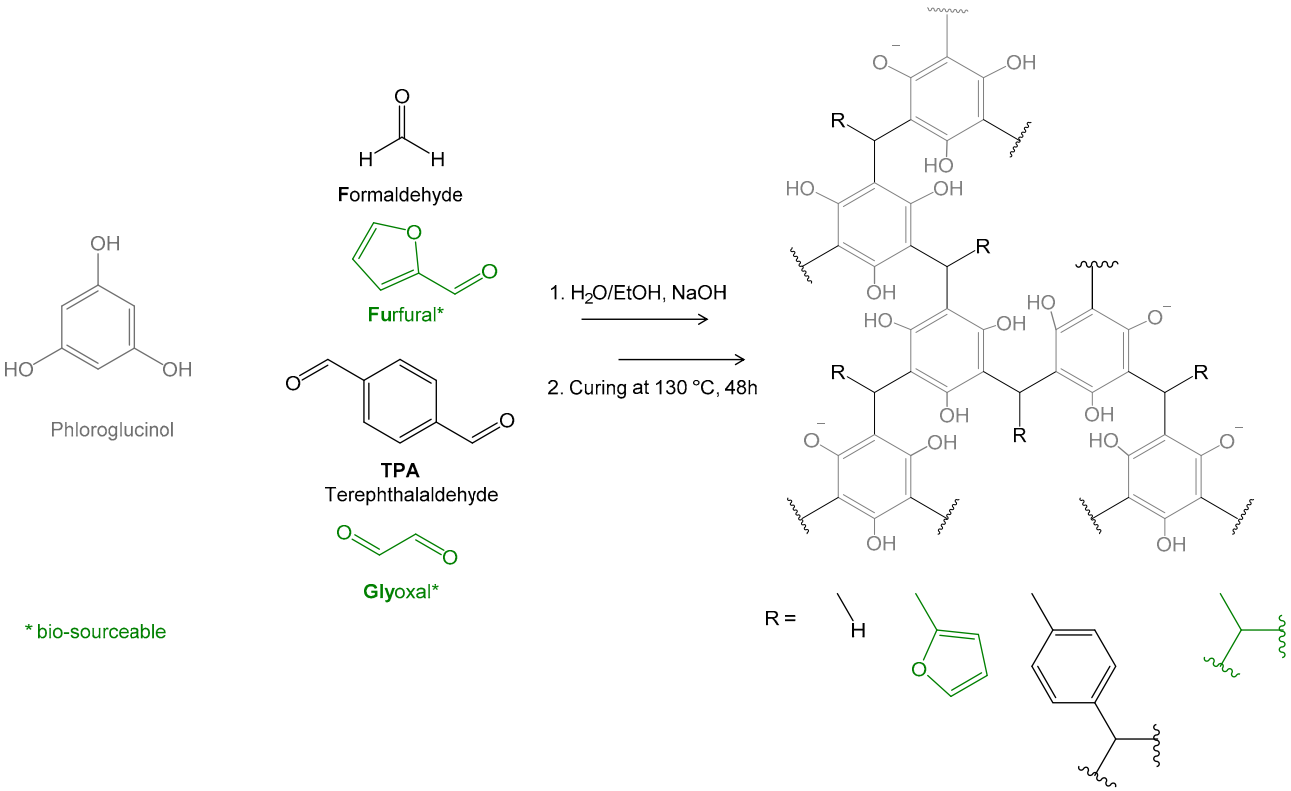

Figure 1. Synthesis pathway of phenolic-like resins.

2.2. Sorption/Desorption Experiments

The properties of resins toward REE adsorption were studied in 0.1 M acetic acid by varying the initial cation concentration, contact time, temperature, pH, and competing metal. Desorption was studied using a hydrochloric acid solution, one of the most suitable acid for REE refining [47], by varying the contact time and acid concentration.

2.2.1. Equilibrium Sorption Isotherm

Sorption isotherms were performed using a mixture of La and Yb in 0.1 M acetic acid to compare the behavior of the resins toward light and heavy REEs. The concentrations of cations varied from 2.5 to 200 mg/L. For a clearer representation, the isotherm has been plotted as a function of the initial concentration, as shown in Figure 2. The isotherm plotted as a function of the equilibrium concentration is shown in Figure S5. There are no significant differences between light and heavy REEs. The resins Ph-TPA and Ph-Fu showed lower capacities than Ph-F and Ph-Gly, with 30, 33, 50, and 65 mg/g for both cations. A decrease in Qe was observed for the higher initial concentrations, which can be attributed to potential factors such as surface site saturation, competitive adsorption, or aggregation effects at higher concentrations, as have already been observed for such materials [31]. Also, X-EDS analyses (Figure S6) confirmed the presence of cations in the resins after the extraction experiments.

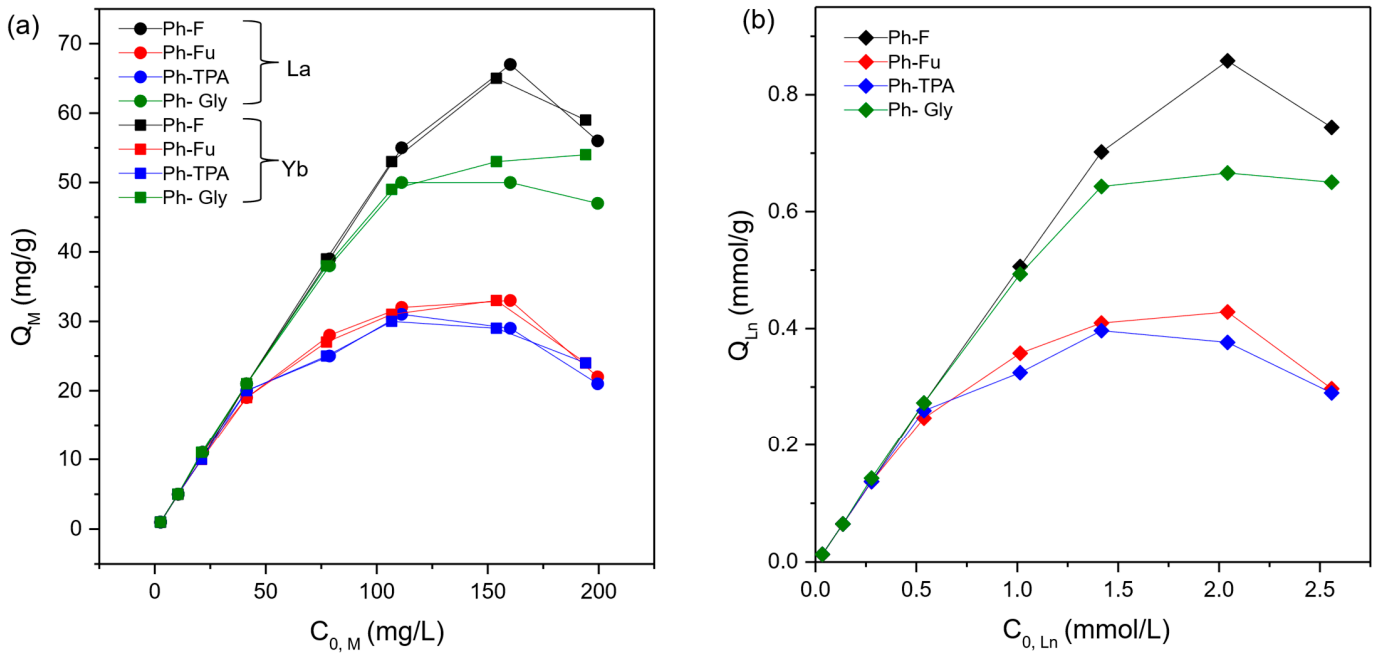

Figure 2. The adsorption isotherms of the resins (Ph-F, Ph-Fu, Ph-TPA, and Ph-Gly) for a mixture of La and Yb in acetic acid (0.1 M, pH = 2.8) at V/m = 0.5 for 16 h at 25 °C. (**a**) The capacity for each metal (M = La or Yb) expressed in mg/g; (**b**) the capacity for both metals (Ln = La and Yb) expressed in mmol/g.

The adsorption behavior of the lanthanides (Lns), specifically La and Yb, either individually or in combination, onto the various resins was evaluated using Langmuir (Figures S7 and S8) and Freundlich (Figure S9) isotherm models. A comparative analysis of the model fittings (Figures S8 and S9) indicated that the Langmuir isotherm provided a more suitable fit. This suggests that it is the most appropriate model for describing the adsorption of La and Yb onto the studied resins. This conclusion is supported by the high linearity and correlation coefficients (R^2) observed in the Langmuir plots, in contrast to the non-linear behavior exhibited by the Freundlich isotherms.

As shown in Figure 2, the Ln adsorption profiles across all resins closely followed the Langmuir model, characterized by rapid uptake at low concentrations, followed by a plateau, with a slight decrease at higher concentrations. This behavior is consistent with mechanisms involving monolayer adsorption on a homogeneous surface [48].

The maximum adsorption capacity of the resins (Q_{max}) was determined from the Langmuir plots (Figure S4) using the slope and intercept of the linearized isotherm equations. The calculated Q_{max} values for Ln ranged from 0.38 to 0.75 mmol/g in the following order: Ph-F (0.75) > Ph-Gly (0.66) > Ph-Fu (0.43) > Ph-TPA (0.38) (Table S1).

The adsorption performance of the synthesized sorbents (Ph-F, Ph-Fu, Ph-TPA, and Ph-Gly) was evaluated and compared with data reported for a variety of commercial resins (Table 1). Although the maximum adsorption capacities obtained in this study are lower than those of high-capacity sorbents, such as D113 resin [49] and gel-type weak acid resin [50], these results must be interpreted in light of the significantly different experimental conditions under which the adsorption studies were performed. The experiments in this study were carried out at a strongly acidic pH of 2.8. In contrast, most comparative studies were conducted at favorable pH levels ranging from 4.38 to 6.0. Under near-neutral conditions, the availability of binding sites for metal ions increases due to the lower concentration of competing protons (H^+). However, in highly acidic media, proton competition for active sites becomes more intense, often leading to decreased metal ion uptake.

Table 1. Comparison of the obtained results with commercial sorbents for La(III) and Yb (III) sorption from organic acid medium.

Sorbent	Acid Medium	Max Capacity (mg/g)	Reference
D113 resin	Acetate buffer (pH = 6)	273.3 (La^{3+})	Shu et al. [49]
Gel-type weak acid resin (110)	Acetate buffer (pH = 5.50)	265.8 (Yb^{3+})	Zheng et al. [50]
Diphonix Resin® Purolite S957	Citric acid (pH = 6)	60.01 (La^{3+}) 58.35 (La^{3+})	Araucz et al. [51]
Amberlite IRC86	Acetic-acid-buffered media (pH = 4.38)	40.56 (La^{3+})	Bezzina et al. [52]
Ph-F	Acetic acid (pH = 2.8)	56.91 (La^{3+}) 59.35 (Yb^{3+})	This work
Ph-Fu		33.14 (La^{3+}) 32.84 (Yb^{3+})	
Ph-TPA		29.04 (La^{3+}) 29.06 (Yb^{3+})	
Ph-Gly		47.68 (La^{3+}) 54.02 (Yb^{3+})	

Despite the challenging pH conditions, the synthesized sorbents exhibited significant adsorption capacities. For example, Ph-F and Ph-Gly displayed maximum capacities of 56.91 and 47.68 mg/g for La^{3+}, respectively, and 59.35 and 54.02 mg/g for Yb^{3+}, respectively. Ph-Fu and Ph-TPA also exhibited consistent performance. Notably, these values are similar to those reported for commonly used commercial sorbents, such as Diphonix Resin® (60.01 mg/g for La^{3+}), Purolite S957 (58.35 mg/g for La^{3+}) [51], and Amberlite IRC86 (40.56 mg/g for La^{3+}) [52]. These commercial sorbents were tested under less acidic conditions.

Thus, while the maximum capacities reported in this study are not the highest, the effectiveness of the synthesized sorbents at pH 2.8 highlights their potential as viable alternatives for metal ion recovery in highly acidic environments. Their robustness under such stringent conditions makes them promising candidates for practical applications.

2.2.2. Kinetic Studies

Kinetic studies were performed for the sorption and desorption of a mixture of La and Yb, as previously performed for the isotherms. The adsorption process was meticulously monitored by observing the immediate effect of the acetic acid solution on the activated resins. This observation continued for a period of one day, as depicted in Figure 3a. All materials exhibited rapid kinetic exchange for cations (Na to Ln), yet certain observations merit attention. It was observed that Ph-F and Ph-Gly achieved equilibrium within ten minutes. However, Ph-Fu exhibited a slight slowdown prior to reaching the plateau, while Ph-TPA demonstrated a modest decline in adsorption capacity. Nevertheless, equilibrium was achieved for all materials after two hours (black dashed line), with no significant differences observed in the La and Yb concentrations.

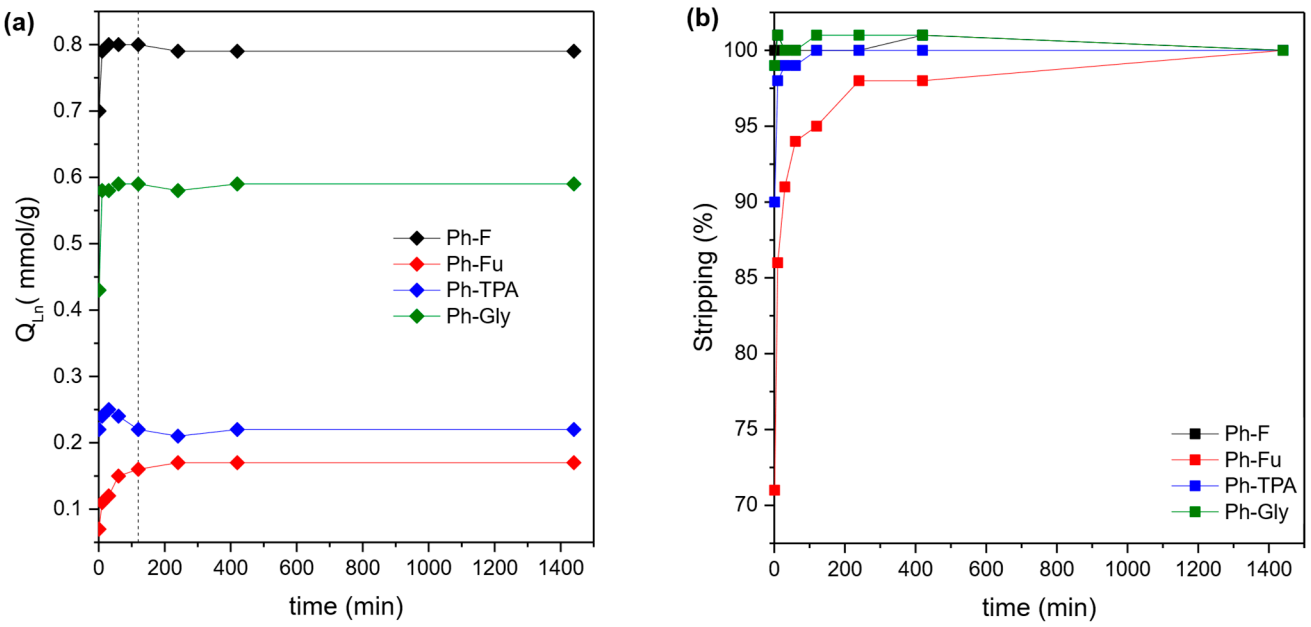

Figure 3. Kinetic analysis of the following: (**a**) The adsorption of a mixture of La (152 ppm) and Yb (196 ppm) in 0.1 M acetic acid (pH = 2.8); V/m = 0.5; t = 1, 10, 30, 60, 120, 240, 420, 1440 min; at 25 °C. (**b**) The back-extraction of La and Yb in a 1 M HCl solution, V/m = 0.5.

The rapid rate of adsorption observed in this experiment does not permit the utilization of the pseudo-first- or pseudo-second-order model. However, the rapid saturation of the adsorbent, which results in a precise line-up, suggests a chemisorption process in which all exchange sites are identical (pseudo-second-order).

Subsequent to the adsorption stage, identical samples were utilized to perform desorption kinetic experiments using a 1 M HCl solution (Figure 3b). A small quantity of solution was extracted from the batch experiments in order to quantify the amount of REEs released. As was the case with the adsorption process, the kinetics of release are extremely rapid for all materials. Full recovery of cations was observed after ten minutes, with the exception of Ph-Fu, which achieved 95% after two hours.

Furthermore, the efficiency of the back-extraction process was examined by varying the HCl concentration, with the objective of investigating the feasibility of implementing a less acidic solution (Figure S10). The absence of desorption when using H_2O exclusively indicates the feasibility of resin washing prior to REE recovery. The solution at 0.01 M facilitated the recovery of 43 to 56% of the adsorbed cations, 10-1 M resulted in 75–88% recovery, and 0.5 M yielded BE > 90%, while quantitative recovery was obtained with 1 M HCl. As demonstrated in Figure S11, the sorption and stripping capabilities of the sorbent remained high. This was observed even after two sorption/stripping cycles had been completed.

2.2.3. Influence of Temperature

In order to assess the influence of temperature on the adsorption process, extraction experiments were conducted with a mixture of La and Yb in acetic acid at temperatures ranging from 20 °C to 50 °C (Figure 4). After a two-hour period, no substantial alterations were detected, except in the case of Phy-Gly, where a slight increase as temperature rises in terms of adsorption capacity or selectivity between light and heavy REEs was observed.

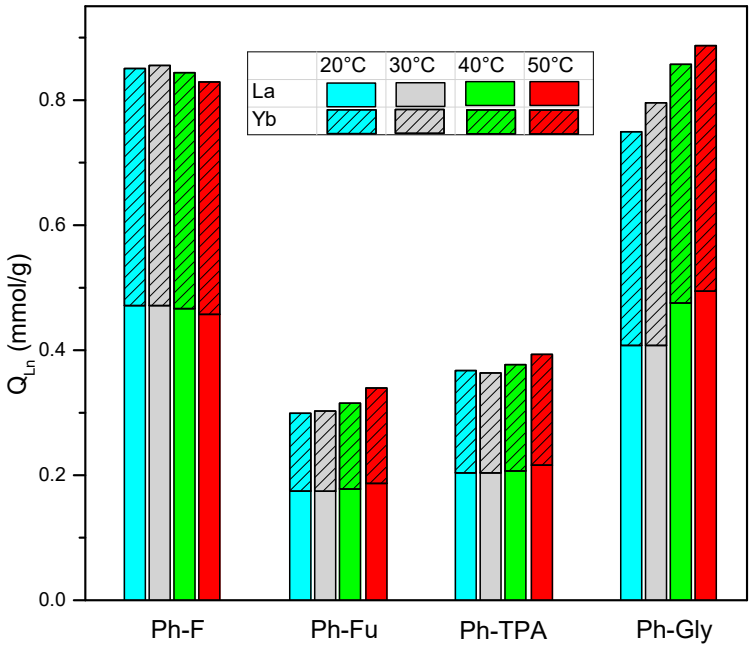

Figure 4. The adsorption capacity of the sorbents for a mixture of La and Yb in acetic acid 0.1 M (pH = 2.8) as a function of temperature. V/m = 0.5, contact time = 2 h.

Adsorption is a multifaceted process involving two distinct mechanisms: (i) the desorption of solvent molecules (e.g., water, acetic acid) and (ii) the adsorption of adsorbate on the surface (in this case, an exchange with Na^+) [53]. According to the Gibb free energy (ΔG0) equation, the spontaneity of a process can be determined by its relationship to enthalpy (ΔH0), entropy (ΔS0), and temperature (T) [54]. The experimental findings suggest that the sorption process is spontaneous and does not require energy input, at least at temperatures below 20 °C. Accordingly, in the context of Gibbs free energy, the value is negative, indicating that the exothermicity of cation exchange exceeds the energy required to denude the metal solvent sheath in solution. This phenomenon results in an adsorption capacity that remains temperature-independent.

2.2.4. Selectivity Towards Competing Metals

An investigation was conducted into the selectivity of the process towards scandium (Sc), iron (Fe), and aluminum (Al), given their prevalence as competitors in leaching solutions [55]. The presence of all three metals was identified in red mud leachates, with Fe emerging as the predominant competitor in permanent magnet leachate. In the course of these experiments, the effect of pH solution on selectivity was also investigated. Experiments were conducted at pH values of 2, 3, 4, and 5 (Figure 5). At a pH level below 2, there is a significant decrease in adsorption capacity. Conversely, at a pH level above 5, the process of metal hydroxide precipitation may interfere with the desired outcome. The extraction results demonstrated significant variations in the behavior of the materials, with a notable impact of pH on both adsorption capacity and selectivity.

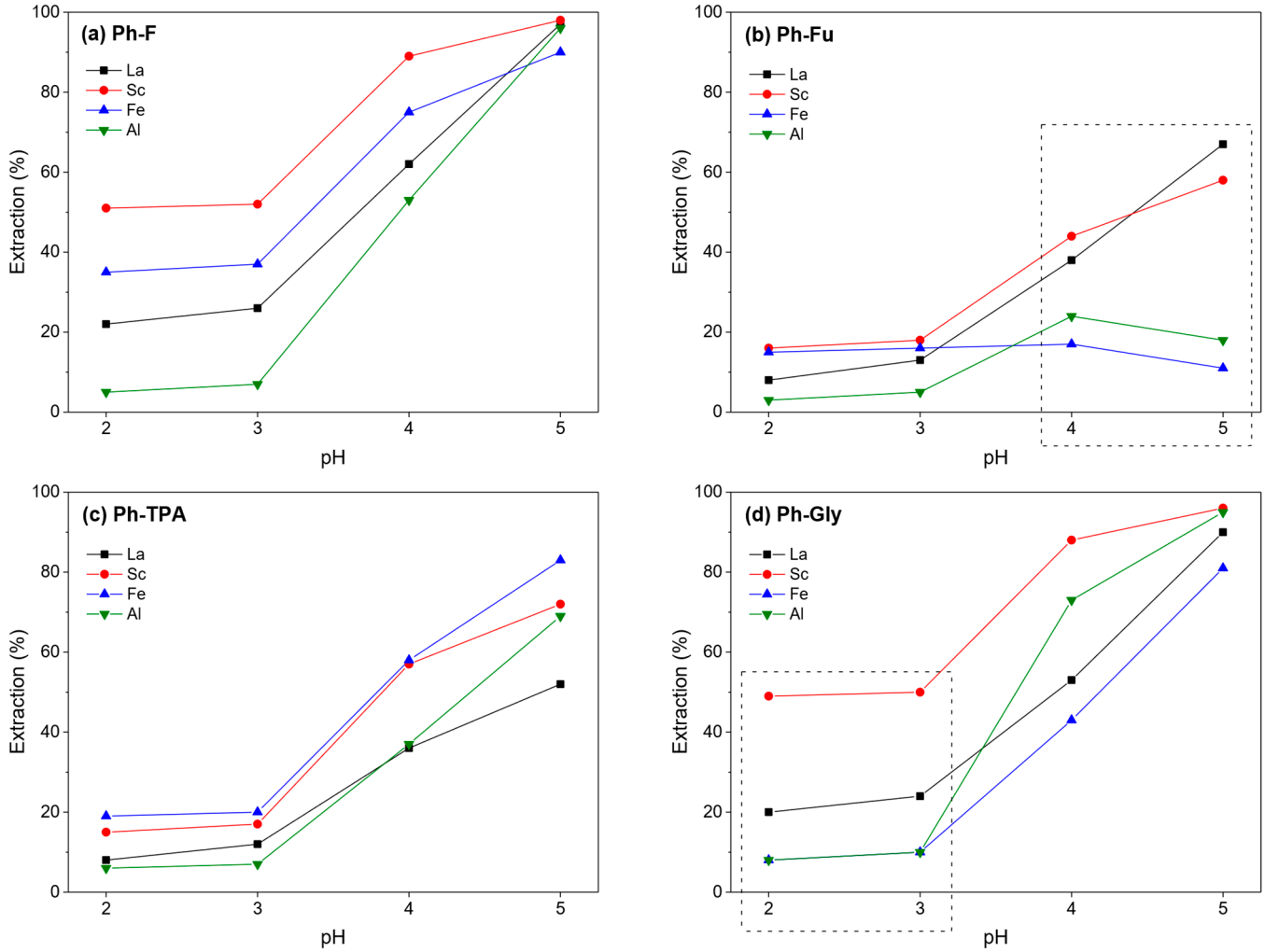

Figure 5. Extraction efficiencies (%) of sorbents for La, Sc, Fe, and Al from acetic acid solution as function of pH. Conditions: Al, Fe, Sc, La (≈50 ppm), acetic acid solution (pH adjusted with HCl or NaOH), V/m = 0.5, contact time = 4 h at 25 °C.

The observed disparities in selectivity among the various sorbent materials can be primarily attributed to differences in the accessibility and distribution of hydroxyl functional groups, which arise from the specific structural arrangements formed during the polymerization of phloroglucinol. These structural variations are, in turn, strongly influenced by the nature and reactivity of the aldehyde co-monomers employed in the synthesis. The type of aldehyde dictates not only the crosslinking density and spatial orientation of the polymer network, but also modulates the exposure of hydroxyl sites. These sites are critical for selective interactions with target analytes during sorption processes.

As was previously demonstrated in the sorption isotherm analysis at a pH of 2.8, the extraction percentage exhibited the following sequence: Ph-F ≥ Ph-Gly >> Ph-TPA ≥ Ph-Fu. Extraction at pH values of 4 and 5 resulted in a substantial enhancement of extraction, as illustrated in Figure S12. It has been demonstrated that all of the resins exhibit the capacity to extract metal at a rate that is twice that of Ph-Fu and up to four times that of the other materials at pH = 5. This trend in extraction capacity can be attributed primarily to the decline in H^+ concentration, leading to a reduction in the competition between the protonation of activated alcoholate function and metal chelation. Furthermore, acetic acid has a pKa constant of 4.8. Consequently, a mixture of acid and acetate exists at a pH of 4–5. This significantly impacts the selectivity between the four metals in solution (Table S2). The observed alterations can be attributed to the thermodynamic constant of metal–acetate

complexes, which exhibit significant variation. This variation has a substantial impact on the selectivity of the system when the pH of the solution is altered. Notably, two resins have been identified as being particularly noteworthy within the range of pH values examined (Table 2). The Ph-Gly adsorbent demonstrates notable efficacy in extraction operations conducted at pH values ranging from 2 to 3, exhibiting a separation factor of approximately 3. This performance is particularly evident in the context of $SF_{La/Fe}$, which is observed to be lower in comparison to alternative resins. The adsorbent Ph-Fu exhibits remarkable efficacy in the separation process at pH values ranging from 4 to 5, exhibiting a substantially higher SF compared to other adsorbents, particularly $SF_{La/Fe}$, with an SF value exceeding 16 at a pH of 5.

Table 2. Separation factor (SF) for Ph-Gly at pH = 2, 3 and Ph-Fu at pH = 4, 5. All values available in Table S2.

	Ph-Gly				**Ph-Fu**		
pH	**$SF_{Sc/La}$**	**$SF_{La/Fe}$**	**$SF_{La/Al}$**	**pH**	**$SF_{Sc/La}$**	**$SF_{La/Fe}$**	**$SF_{La/Al}$**
2	3.7	2.9	2.8	4	1.3	3.0	1.9
3	3.2	2.9	2.8	5	0.7	16.6	9.4

2.3. Extraction in Real Leachates

This section of the study evaluates the efficiency and selectivity with which the sorbents extract metal ions in real leachates, such as those found in permanent magnets or red mud. The study particularly focuses on their ability to discriminate between REEs (Nd, Pr, and Dy) and common transition metals, particularly Fe.

An aqueous solution was obtained through the lixiviation of permanent magnet powder by 1.6 mol/L acetic acid. This solution was then contacted with four sorbents (Ph-F, Ph-Gly, Ph-Fu, and Ph-TPA) under identical extraction conditions (pH, volume-to-mass ratio, time, and temperature).

The extraction efficiencies and selectivities obtained with the different sorbents are summarized in Figure 6. The sorbent Ph-F demonstrated high extraction efficiencies for REEs (approximately 70%), along with strong selectivity for lanthanides over cobalt and nickel, with selectivity factors ($SF_{Ln/Co}$ and $SF_{Ln/Ni}$) of 11.1 and 10.9, respectively. Additionally, it exhibited an iron selectivity of $SF_{Ln/Fe}$ =3.7. Conversely, Ph-Fu exhibited moderate extraction of lanthanides, with efficiencies approaching 30%, and notably diminished selectivity, as evidenced by $SF_{Ln/Co}$ and $SF_{Ln/Ni}$ values of 2.0 and 2.1, respectively. However, its selectivity towards iron is much more pronounced, with a value of 8.9. The Ph-Gly sorbent exhibited balanced performance, achieving moderate REE extraction (approximately 50%) and exhibiting good selectivity over iron, with a selectivity factor $SF_{Ln/Fe}$ of 5.2. The extraction efficiencies of Ph-TPA were found to be marginally lower than those of Ph-Gly. However, Ph-TPA demonstrated acceptable selectivity, particularly in the context of cobalt (SFLn/Co = 3.9). Across all sorbents, iron consistently exhibited lower extraction, thereby underscoring the observed sorbents' preference for lanthanides over transition metals. These findings highlight the potential of the sorbents in developing efficient separation process for REEs from complex metal mixtures such as an acetic acid leachate of permanent magnets.

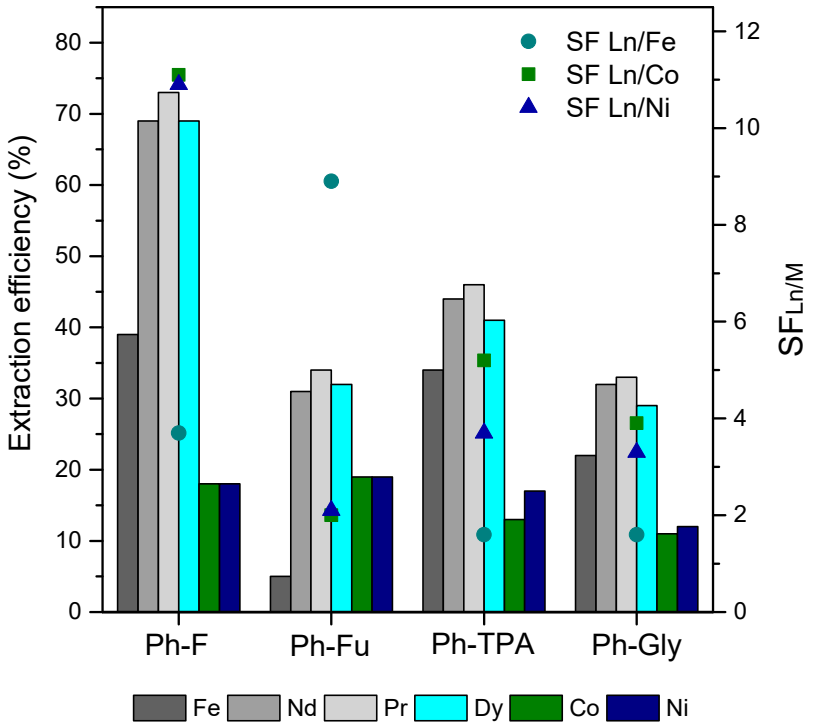

Figure 6. Extraction efficiency (%) of sorbents for Fe, Nd, Pr, Dy, Co, and Ni, as well as corresponding selectivity factors: $SF_{Ln/Fe}$, $SF_{Ln/Co}$, $SF_{Ln/Ni}$. Conditions: Fe^{3+} = 1536 mg/L, Nd^{3+} = 1006 mg/L, Pr^{3+} = 155 mg/L, Dy^{3+} = 58 mg/L, Co^{3+} = 56 mg/L, Ni^{2+} = 12 mg/L in acetic acid (1.6 mol/L, pH = 3), V/m = 0.1, contact time = 2 h at 25 °C.

A subsequent series of experiments was conducted to assess the extraction performance of sorbents in the context of an organic acid red mud leachate (Table S3). Red mud leachates were prepared using citric, lactic, and acetic acids as leaching agents to simulate environmentally relevant extraction conditions. These leachates were subsequently subjected to sorption experiments employing functionalized resins: Ph-F in both hydroxyl (-OH) and sodium (-ONa) forms, and Ph-Gly in the sodium form (-ONa). The Ph-Gly resin was evaluated under two different volume-to-mass ratios, specifically V/m = 0.2 and 0.5, to assess the influence of solid-to-liquid contact conditions on extraction efficiency.

The nature of the acid employed in the leaching process plays a crucial role in determining the extent to which metals form complexes in solution, which directly influences their availability for subsequent sorption. Among the acids studied—citric, lactic, and acetic—there are notable differences in their complexing strengths due to their molecular structures.

Citric acid, with its tricarboxylic structure, has been shown to form strong complexes with trivalent metal ions, including Fe^{3+}, Al^{3+}, and rare earth elements (REEs). This high affinity is attributed to its multiple coordination sites (three carboxylic acid groups and one hydroxyl group), which allow it to chelate metals efficiently and stabilize them in solution [56]. Lactic acid, in contrast, is classified as an alpha-hydroxy acid, bearing a carboxylic group and a hydroxyl group. It has been observed to form moderately strong complexes with metal ions, thereby offering a certain degree of stabilization, although not to the same extent as citric acid. Its simpler structure results in a limited number of coordination interactions that can be established with metal ions. Acetic acid demonstrates the weakest complexation behavior among the three acids studied. The presence of a single carboxyl group confers limited binding capacity, leading to a greater proportion of "free" metal ions remaining in solution. This lower complexation strength can influence the sorption process, as metals are more readily available for direct interaction with sorbents.

The general trend in complexation strength with REEs is citric acid > lactic acid > acetic acid, which aligns with their molecular structures and number of coordination sites [57]. Consequently, the availability of metals for the sorption process is reversed. This observation is corroborated by the results presented in Figure S13, which demonstrate extraction efficiency, with maximum extraction percentages of approximately 10% for citric acid, 40% for lactic acid, and 60% for acetic acid.

It is evident across the three leaching systems that metal speciation in solution is the primary determinant of sorption efficiency. While citric acid is an excellent leachant, it creates metal complexes that are too stable for recovery via conventional resins. Lactic acid occupies an intermediate position, whereas acetic acid produces leachates that are rich in "free" or "labile" metal ions, which are optimal for sorption. These considerations must be taken into account in the context of selectivity for REEs, as this is more pronounced when sorption is performed from a lactic acid leachate. From a materials standpoint, the sodium-exchanged form of the phenolic resin (Ph-F-ONa) exhibited high and consistent performance, thanks to its efficient ion-exchange capacity. In contrast, the glyoxal-crosslinked variants (Ph-Gly-ONa) only demonstrated increased extraction under favorable conditions (acetic acid leachate). This suggests that crosslinking enhances physical properties, such as stability and swelling, rather than directly contributing to chemical affinity for metal ions. Over-crosslinking can reduce extraction efficiency by limiting diffusion and site availability.

The data on extraction efficiency obtained in citric, lactic, and acetic acid media demonstrate a distinct selectivity of the synthesized sorbents towards REEs over Al^{3+}, despite potential concerns regarding aluminum leaching. In particular, lactic acid solutions yielded the most pronounced differentiation, with REE extraction efficiencies reaching up to 40%, while Al^{3+} uptake remained consistently below 10% across all sorbents. These findings suggest that Al^{3+} does not exhibit competitive inhibition of REE sorption under the experimental conditions, thereby validating the sorbents' affinity for REEs in environments that are weakly to moderately complexing.

3. Materials and Methods

3.1. Chemicals

All obtained chemicals were analytically pure from Sigma–Aldrich (Saint Quentin Fallavier, France) or Thermo Fisher (Illkirch, France) and used without further purification: acetic acid (99%), phloroglucinol (99%), furfural (99%), terephthalaldehyde (98%), glyoxal (40% in water), and formaldehyde (37% in water). The ICP standards were purchased from SCP Science (Villebon-sur-Yvette, France).

3.2. General Procedure for Resin Synthesis

Phloroglucinol and sodium hydroxide (NaOH) pellets (0.5 eq.) were dissolved in a mixture of H_2O/EtOH (v/v with 50 eq. H_2O). Aldehyde (3 eq. Formaldehyde, 2 eq. Furfural, 1 eq. Glyoxal, or 1 eq. Terephthalaldehyde TPA) was added, and the reaction mixture was stirred overnight. Then, it was transferred to a crystallizer and cured in a ventilated oven at 130 °C for 48 h. The resulting solid, tough resin was recovered and ground using a ball mill for 15 min at 25 Hz. It was then washed with NaOH (1 M), HCl (1 M), and H_2O to obtain the protonated -OH form. The washed resins were then dried in a ventilated oven at 80 °C for 24 h, quickly dispersed by ball milling, and stored for extraction experiments. Before each experiment, the resins were activated using 0.1 M NaOH (0.5 mL/mg), then rinsed once with H_2O.

3.3. Characterization Techniques for Resins

The ^{13}C solid-state MAS NMR spectra were recorded at a rotation speed of 12 kHz (using 4 mm outer-diameter rotors) with a Bruker Advance 400 MHz spectrometer (Brucker, Wissembourg, France). The resins were mechanically ground at 25 Hz for 15 min using a Retsch mixer mill MM 200 (Retsch, Eragny sur Oise, France) with a Zr ball. Thermogravimetric analysis (TGA) was performed using a Mettler Toledo instrument (Mettler Toledo, Viroflay, France)with an air or nitrogen flow and a heating rate of 10 °C/min from 25 to 950 °C. An isothermal treatment of 30 min at 100 °C was performed under air to determine the resins' moisture regain from storage. Fourier transform infrared (FTIR) absorption spectroscopy was carried out on a PerkinElmer 100 spectrometer (Perkin Elmer, Villebon S/Yvette, France) between 615 and 4000 cm^{-1} using an attenuated total reflectance (ATR) crystal with a resolution of 4 cm^{-1}. Scanning electron microscopy (SEM) was performed using a Quattro ESEM instrument (ThermoScientific, Les Ulis, France) coupled with a XFlash6 / 100 Energy Dispersive X-ray Spectrometer with Quantax 400 software (Bruker, Wissembourg, France) (SEM/EDS) to study the morphology of the resins. Metal ion concentrations before and after sorption were determined using inductively coupled plasma/atomic emission spectroscopy (ThermoScientific, ICAP 7000 series; ThermoScientific, Les Ulis, France). The wavelengths used for Al, Fe, Sc, La, and Yb measurements were chosen to avoid spectral interference between the elements. The red mud leachates were quantified before and after sorption using inductively coupled plasma mass spectrometry (ICP-MS, PerkinElmer 300X Quadrupole; Perkin Elmer, Villebon S/Yvette, France).

3.4. Batch Extraction

A series of metal solutions were prepared for the sorption experiments, including a solution of La, a solution of Yb, and a solution of La and Yb in 0.1 mol/L acetic acid, which was prepared from the salts in their nitrate form, as well as a multicomponent solution containing Al, Fe, Sc, and La (50 mg/L of each element) in 0.1 mol/L acetic acid, with pH adjusted to 2, 3, 4, or 5 using HCl or NaOH.

A permanent magnet leaching solution was prepared from NdFeB magnet powder in acetic acid, as previously described in the literature [12,58].

A red mud leaching solution was prepared according to the literature protocol [15,16], employing organic acids including citric, lactic, and acetic acids. Typically, the leaching of 800 mg of a karstic bauxite residue from France [5] in 40 mL of organic acid was carried out in a microwave at 70 °C for 30 min. The resulting leachate was then filtered through a 0.22 µm filter to remove any remaining bauxite residue particles.

The ability of the thermosetting resins to extract REEs and competing metals was assessed by extraction tests, which were carried out in batch experiments using aqueous solutions. In these experiments, a known amount of resin was activated using a 0.1 M NaOH solution (V/m = 1), then washed with water and dried under air at 100 °C for 12 h. Then the resins were brought into contact with a volume of solution containing metal cations, typically 4 to 6 mg of resin brought into contact with 2 to 3 mL of aqueous solution (V/m = 0.5).

The mixture was stirred at 250 rpm at controlled temperature for a set number of hours, typically at 25 °C for 12 h. After contact, the mixture was centrifuged. The supernatant was filtered through a 0.22 µm cellulose acetate membrane and then diluted with 1% HNO_3 to achieve a suitable concentration. The amounts of various cations in the filtrate were analyzed using ICP-OES or ICP-MS.

The measured values led to the following:

- The cation uptake capacity Q_{ads} (mg/g) was calculated using the following equation:

$$Q_{ads} = \left(C_i - C_f\right) \cdot \frac{V}{m} \quad (1)$$

with C_i being the initial concentration of the metal ion in solution, C_f the residual metal ion concentration, and V/m the ratio of solution volume by resin-mass.

- The adsorption efficiency E (%) was calculated according to the following equation:

$$E = \frac{C_i - C_f}{C_i} \cdot 100 \quad (2)$$

- The distribution coefficient (K_D), expressed in mL/g, represents the ratio of the number of cations that the resin absorbs to the number of cations that remain in the solution after extraction. It was determined using the following formula:

$$K_D = \frac{C_i - C_f}{C_f} \cdot \frac{V}{m} \cdot 1000 \quad (3)$$

- The separation factor ($FS_{M1/M2}$) is defined as the ratio of the distribution coefficient of metal M1 to that of metal M2, the competing metal ion. This factor quantitatively expresses the selectivity of the resin for metal M1 in the presence of a competing species. The separation factor was calculated using the following equation:

$$FS_{M1/M2} = \frac{K_{D_{M1}}}{K_{D_{M2}}} \quad (4)$$

- The back-extraction or stripping efficiency S (%) is defined by the following equation:

$$S = \frac{Q_e - Q_f}{Q_e} \cdot 100 \quad (5)$$

with Q_e being the concentration of the metal ion loaded into the polymer and Q_f the residual metal ion concentration in the polymer after the release.

Langmuir isotherm parameters [59,60] were estimated by the following equation:

$$\frac{C_e}{Q_e} = \frac{1}{K_L Q_{max}} + \frac{1}{Q_{max}} \cdot C_e \quad (6)$$

with C_e being the concentration of the metal ion in solution at equilibrium, Q_e the amount of metal ion adsorbed at equilibrium, Q_{max} the maximum amount of metal ion adsorbed at equilibrium, and K_L the Langmuir constant. The maximum sorption capacity could be estimated from this isotherm when a plateau was obtained [61].

Freundlich isotherm [62] parameters were estimated by the following equation:

$$\log Q_e = \log K_F + \frac{1}{n} \cdot \log C_e \quad (7)$$

with C_e being the concentration of the metal ion in solution at equilibrium, Q_e the amount of metal ion adsorbed at equilibrium, and K_F and n Freundlich parameters.

3.5. Adsorption Kinetic

The kinetics data were fitted using pseudo-first-order and pseudo-second-order kinetic models [63,64]. The pseudo-first-order model, which is based on solid sorption capacity and was suggested by Lagergren, describes the adsorption phenomenon as a diffusion-

controlled process. In the concentration range studied, this model suggests the formation of monolayer coverage of the adsorbate on the surface of the adsorbent [65,66]. This model was used to describe the sorption kinetics [67–69].

The pseudo-first-order rate is given as

$$\log(Q_e - Q_t) = \log Q_e - \frac{K_1}{2.303} \cdot t \quad (8)$$

where Q_e is the equilibrium metal ion concentration in the solid phase (mg/g), Q_t is the equilibrium metal ion concentration in the solid phase at time t (mg/g), K_1 is the pseudo-first-order equilibrium rate constant (min^{-1}), and t is the time (min).

The pseudo-second-order model is also based on solid-phase adsorption capacity but controlled by the sorption/desorption process and diffusion toward chelating sites [70–72].

The pseudo-second-order rate is given as

$$\frac{t}{Q_t} = \frac{1}{Q_e} \cdot t + \frac{1}{K_2 Q_e^2} \quad (9)$$

where Q_e is the equilibrium metal ion concentration in the solid phase (mg/g), Q_t is the equilibrium metal ion concentration in the solid phase at time t (mg/g), K_2 is the pseudo-first-order equilibrium rate constant (min^{-1}), and t is the time (min).

4. Conclusions

A series of four formo-phenolic-type resins were synthesized by replacing the phenol group with a phloroglucinol group, a biosourceable and biocompatible compound. The synthesis involved the use of four aldehydes or dialdehydes, with two of these aldehydes being produced from biomass, specifically furaldehyde and glyoxal. The isotherms study demonstrated that the resins comply with the Langmuir model, characterized by monolayer chemisorption on equal sites. The maximum adsorption capacity for Ln exhibited a range from 0.38 to 0.75 mmol/g, with Ph-F > Ph-Gly > Ph-Fu > Ph-TPA. The extraction capacity under consideration is independent of temperature (a minimum of 20 °C) but exhibits minimal dependence on the pH of the extraction medium. The extraction capacity is up to fourfold greater when the pH range is from 2 to 5. The rate of extraction is fast, with equilibrium largely reached after two hours. Furthermore, back-extraction is even faster, with the total recovery of metal after ten minutes in HCl 1M.

For instance, the selectivity of adsorption capacity exhibits a substantial variation in accordance with the pH level. It is noteworthy that the two resins demonstrating optimal separation properties are those polymerized using biosourceable aldehydes, specifically glyoxal at a pH of 2–3 and furfural at a pH of 3–4.

In order to assess the efficacy of resins in a real-life environment, an extraction process was conducted on permanent magnet leachate in 1.6 M acetic acid. This extraction process yielded highly promising results, with lanthanides being extracted from 30% to 70% and the selective extraction of lanthanides over Fe, Co, and Ni with from 2 up to 10 depending on the sorbent and the metal considered. This comparative study demonstrates that Ph-F and Ph-Gly are promising candidates for selective REE recovery from complex metal mixtures such as acetic acid leachates of permanent magnets.

A final experiment was conducted on red mud leachate, which demonstrated the efficacy of resins in diluted media. The results of this study demonstrate the crucial interplay between leachate chemistry and sorbent functionality in determining the efficiency of metal recovery from red mud. While the use of acetic acid resulted in the significant extraction of REEs due to the weak coordination environment it creates, the application of stronger complexing agents such as citric and lactic acid led to poor recovery, particularly for

REEs. This suggests that standard phenolic-based sorbents, even when crosslinked with glyoxal, lack sufficient affinity to displace stable organic complexes in solution. To address this limitation, future work should explore the incorporation of selective chelating ligands directly into the polymeric matrix of the sorbent. Ideally, these ligands should exhibit higher complexation stability constants for REEs and transition metals than common organic acids, enabling competitive displacement and capture. Finally, combining this ligand-driven approach with smart regeneration strategies, such as pH switching, competitive stripping, and selective elution using mild chelators, could enable closed-loop, sustainable processes for recovering critical metals from red mud and other bauxite residues.

Supplementary Materials: The following supporting information can be downloaded at: https://www.mdpi.com/article/10.3390/recycling10040165/s1, Figure S1: ^{13}C solid-state NMR of resins; Figure S2: FT-IR spectra of resins; Figure S3: Thermogravimetric analysis of resins; Figure S4: SEM image of resin Ph-Gly; Figure S5: Adsorption isotherms of the resins; Figure S6: X-EDS spectra of resin Ph-Gly after extraction; Figure S7: Plot of the Langmuir isotherm equation for Ln (La+Yb) adsorption; Figure S8: Plot of the Langmuir isotherm equation for La or Yb adsorption; Figure S9: Plot of Freundlich isotherm equation for La or Yb adsorption; Figure S10: Back-extraction efficiency (%), loaded sorbent; Figure S11: Sorption and stripping cycle; Figure S12: Adsorption capacity for the sorbent as function of pH; Figure S13: Extraction efficiencies (%) of the sorbents for red mud leachates; Table S1: Maximum adsorption capacity and Langmuir constant; Table S2: Separation factor (SF) for the sorbent as a function of pH; Table S3: Composition of red mud leachates.

Author Contributions: E.L. (Conceptualization, Methodology, Investigation, Data Curation, Writing—Original Draft), J.C. (Conceptualization, Methodology), C.L. (Conceptualization, Methodology, Project Administration, Funding Acquisition), S.P.-R. (Conceptualization, Methodology, Supervision), G.A. (Conceptualization, Methodology, Writing—Review and Editing, Supervision, Project Administration, Funding Acquisition). All authors have read and agreed to the published version of the manuscript.

Funding: The authors acknowledge financial support from the CNRS through the MITI interdisciplinary program (PRIME 2020: ExtraMet project) and the French Agence Nationale de la Recherche through the RECALL project (ANR-20-CE04-0007).

Data Availability Statement: The original contributions presented in this study are included in the article/supplementary material. Further inquiries can be directed to the corresponding author.

Acknowledgments: The authors would like to thank C. Rey, J. Lautru, B. Baus-Lagarde, and B. Angeletti for their assistance in conducting TGA, SEM-EDS, ICP-OES, and ICP-MS analyses, respectively.

Conflicts of Interest: The authors declare that they have no known competing financial interests or personal relationships that could have appeared to influence the work reported in this paper.

References

1. Reisman, D.; Weber, R.; Mckernan, J.; Northeim, C.; U.S. Environmental Protection Agency. *Rare Earth Elements: A Review of Production, Processing, Recycling and Associated Environmental Issues*; United States Environmental Protection Agency: Washington, DC, USA, 2013.
2. Grohol, M.; Veeh, C. *Study on the Critical Raw Materials for the EU 2023—Final Report*; European Commission; Publications Office of the European Union: Luxembourg, 2023.
3. Binnemans, K.; Jones, P.T.; Blanpain, B.; Van Gerven, T.; Yang, Y.; Walton, A.; Buchert, M. Recycling of Rare Earths: A Critical Review. *J. Clean. Prod.* **2013**, *51*, 1–22. [CrossRef]
4. Jowitt, S.; Werner, T.; Weng, Z.; Mudd, G. Recycling of the Rare Earth Elements. *Curr. Opin. Green Sustain. Chem.* **2018**, *13*, 1–7. [CrossRef]
5. Couturier, J.; Oularé, P.T.; Collin, B.; Lallemand, C.; Kieffer, I.; Longerey, J.; Chaurand, P.; Rose, J.; Borschneck, D.; Angeletti, B.; et al. Yttrium Speciation Variability in Bauxite Residues of Various Origins, Ages and Storage Conditions. *J. Hazard. Mater.* **2024**, *464*, 132941. [CrossRef]

6. Deady, É.; Mouchos, E.; Goodenough, K.; Williamson, B.; Wall, F. Rare Earth Elements in Karst-Bauxites: A Novel Untapped European Resource? In Proceedings of the ERES 2014: 1st conference on European Rare Earth Resources, Milos, Greece, 4–7 September 2014.
7. Liu, Y.; Naidu, R. Hidden Values in Bauxite Residue (Red Mud): Recovery of Metals. *Waste Manag.* **2014**, *34*, 2662–2673. [CrossRef] [PubMed]
8. Akcil, A.; Akhmadiyeva, N.; Abdulvaliyev, R.; Abhilash; Meshram, P. Overview On Extraction and Separation of Rare Earth Elements from Red Mud: Focus on Scandium. *Miner. Process. Extr. Metall. Rev.* **2018**, *39*, 145–151. [CrossRef]
9. Hidayah, N.N.; Abidin, S.Z. The Evolution of Mineral Processing in Extraction of Rare Earth Elements Using Liquid-Liquid Extraction: A Review. *Miner. Eng.* **2018**, *121*, 146–157. [CrossRef]
10. Zhao, M.; Zhang, H.; Han, H.; Jiang, X.; Yang, Y.; Li, T. Differential Leaching Mechanisms and Ecological Impact of Organic Acids on Ion-Adsorption Type Rare Earth Ores. *Sep. Purif. Technol.* **2025**, *362*, 131701. [CrossRef]
11. Banerjee, R.; Chakladar, S.; Mohanty, A.; Chakravarty, S.; Chattopadhyay, S.K.; Jha, M.K. Review on the Environment Friendly Leaching of Rare Earth Elements from the Secondary Resources Using Organic Acids. *Geosyst. Eng.* **2022**, *25*, 95–115. [CrossRef]
12. Belfqueh, S.; Seron, A.; Chapron, S.; Arrachart, G.; Menad, N. Evaluating Organic Acids as Alternative Leaching Reagents for Rare Earth Elements Recovery from NdFeB Magnets. *J. Rare Earths* **2023**, *41*, 621–631. [CrossRef]
13. Gergoric, M.; Barrier, A.; Retegan, T. Recovery of Rare-Earth Elements from Neodymium Magnet Waste Using Glycolic, Maleic, and Ascorbic Acids Followed by Solvent Extraction. *J. Sustain. Metall.* **2019**, *5*, 85–96. [CrossRef]
14. Gergoric, M.; Ekberg, C.; Foreman, M.R.S.J.; Steenari, B.-M.; Retegan, T. Characterization and Leaching of Neodymium Magnet Waste and Solvent Extraction of the Rare-Earth Elements Using TODGA. *J. Sustain. Metall.* **2017**, *3*, 638–645. [CrossRef]
15. Couturier, J.; Levard, C.; Collin, B.; Chaurand, P.; Vidal, V.; Mathon, O.; Duvivier, A.; Angeletti, B.; Borschneck, D.; Rose, J.; et al. Dissolution of Rare Earth Elements: Exploring the Ability of Deep Eutectic Solvents and Organic Acid Solutions, the Case of Lactic Acid. *Sep. Purif. Technol.* **2025**, *366*, 132740. [CrossRef]
16. Lallemand, C.; Ambrosi, J.; Borschneck, D.; Angeletti, B.; Chaurand, P.; Campos, A.; Desmau, M.; Fehlauer, T.; Auffan, M.; Labille, J.; et al. Potential of Ligand-Promoted Dissolution at Mild pH for the Selective Recovery of Rare Earth Elements in Bauxite Residues. *ACS Sustain. Chem. Eng.* **2022**, *10*, 6942–6951. [CrossRef]
17. Nayl, A.; Arafa, W.; Abd-Elhamid, A.; Elkhashab, R. Studying and Spectral Characterization for the Separation of Lanthanides from Phosphate Ore by Organic and Inorganic Acids. *J. Mater. Res. Technol.* **2020**, *9*, 10276–10290. [CrossRef]
18. Zhang, L.; Chen, H.; Pan, J.; Yang, F.; Long, X.; Yang, Y.; Zhou, C. Rare Earth Elements Recovery and Mechanisms from Coal Fly Ash by Column Leaching Using Citric Acid. *Sep. Purif. Technol.* **2025**, *353*, 128471. [CrossRef]
19. Golzar-Ahmadi, M.; Bahaloo-Horeh, N.; Pourhossein, F.; Norouzi, F.; Schoenberger, N.; Hintersatz, C.; Chakankar, M.; Holuszko, M.; Kaksonen, A. Pathway to Industrial Application of Heterotrophic Organisms in Critical Metals Recycling from E-Waste. *Biotechnol. Adv.* **2024**, *77*, 108438. [CrossRef]
20. Pavón, S.; Fortuny, A.; Coll, M.T.; Sastre, A.M. Rare Earths Separation from Fluorescent Lamp Wastes Using Ionic Liquids as Extractant Agents. *Waste Manag.* **2018**, *82*, 241–248. [CrossRef]
21. Kumari, A.; Sinha, M.K.; Pramanik, S.; Sahu, S.K. Recovery of Rare Earths from Spent NdFeB Magnets of Wind Turbine: Leaching and Kinetic Aspects. *Waste Manag.* **2018**, *75*, 486–498. [CrossRef] [PubMed]
22. Sharifian, S.; Wang, N.-H.L. Resin-Based Approaches for Selective Extraction and Purification of Rare Earth Elements: A Comprehensive Review. *J. Environ. Chem. Eng.* **2024**, *12*, 112402. [CrossRef]
23. Dave, S.R.; Kaur, H.; Menon, S.K. Selective Solid-Phase Extraction of Rare Earth Elements by the Chemically Modified Amberlite XAD-4 Resin with Azacrown Ether. *React. Funct. Polym.* **2010**, *70*, 692–698. [CrossRef]
24. Zereen, F.; Yilmaz, V.; Arslan, Z. Solid Phase Extraction of Rare Earth Elements in Seawater and Estuarine Water with 4-(2-Thiazolylazo) Resorcinol Immobilized Chromosorb 106 for Determination by Inductively Coupled Plasma Mass Spectrometry. *Microchem. J.* **2013**, *110*, 178–184. [CrossRef]
25. Karadaş, C.; Kara, D.; Fisher, A. Determination of Rare Earth Elements in Seawater by Inductively Coupled Plasma Mass Spectrometry with Off-Line Column Preconcentration Using 2,6-Diacetylpyridine Functionalized Amberlite XAD-4. *Anal. Chim. Acta* **2011**, *689*, 184–189. [CrossRef]
26. Ebraheem, K.A.K.; Mubarak, M.S.; Yassien, Z.J.; Khalili, F. Chelation Properties of Poly(8–Hydroxyquinoline 5,7–Diylmethylene) Crosslinked with Bisphenol–A Toward Lanthanum(III), Cerium(III), Neodimium(III), Samarium(III), and Gadolinium(III) Ions. *Sep. Sci. Technol.* **2000**, *35*, 2115–2125. [CrossRef]
27. Draye, M.; Czerwinski, K.; Favre-Réguillon, A.; Foos, J.; Guy, A.; Lemaire, M. Selective Separation of Lanthanides with Phenolic Resins: Extraction Behavior and Thermal Stability. *Sep. Sci. Technol.* **2000**, *35*, 1117–1132. [CrossRef]
28. Al-Rimawi, F.; Ahmad, A.; Khalili, F.; Mubarak, M. Chelation Properties of Some Phenolic-Formaldehyde Polymers toward Some Trivalent Lanthanide Ions. *Solvent Extr. Ion Exch.* **2004**, *22*, 721–735. [CrossRef]
29. Ameta, R.; Patel, V.; Joshi, J. Polychelates of Phenolic Ion-Exchange Resin: Synthesis and Characterization. *Iran. Polym. J.* **2007**, *16*, 615–625.

30. Arrambide, C.; Arrachart, G.; Berthalon, S.; Wehbie, M.; Pellet-Rostaing, S. Extraction and Recovery of Rare Earths by Chelating Phenolic Copolymers Bearing Diglycolamic Acid or Diglycolamide Moieties. *React. Funct. Polym.* **2019**, *142*, 147–158. [CrossRef]
31. Oye Auke, R.; Arrachart, G.; Tavernier, R.; David, G.; Pellet-Rostaing, S. Terephthalaldehyde-Phenolic Resins as a Solid-Phase Extraction System for the Recovery of Rare-Earth Elements. *Polymers* **2022**, *14*, 311. [CrossRef]
32. Liu, Z.; Liu, Y.; Gong, A. Preparation of Diglycolamide Polymer Modified Silica and Its Application as Adsorbent for Rare Earth Ions. *Des. Monomers Polym.* **2019**, *22*, 1–7. [CrossRef]
33. Wilfong, W.C.; Ji, T.; Duan, Y.; Shi, F.; Wang, Q.; Gray, M.L. Critical Review of Functionalized Silica Sorbent Strategies for Selective Extraction of Rare Earth Elements from Acid Mine Drainage. *J. Hazard. Mater.* **2022**, *424*, 127625. [CrossRef]
34. Ginot, L.; El Bakkouche, A.; Giusti, F.; Dourdain, S.; Pellet-Rostaing, S. Hydrophobic Porous Liquids with Controlled Cavity Size and Physico-Chemical Properties. *Adv. Sci.* **2024**, *11*, 2305906. [CrossRef]
35. Brown, A.; Balkus, K. Critical Rare Earth Element Recovery from Coal Ash Using Microsphere Flower Carbon. *ACS Appl. Mater. Interfaces* **2021**, *13*, 48492–48499. [CrossRef] [PubMed]
36. Cardoso, C.E.D.; Almeida, J.C.; Lopes, C.B.; Trindade, T.; Vale, C.; Pereira, E. Recovery of Rare Earth Elements by Carbon-Based Nanomaterials—A Review. *Nanomaterials* **2019**, *9*, 814. [CrossRef]
37. Ashour, R.; Abdelhamid, H.; Abdel-Magied, A.; Abdel-Khalek, A.; Ali, M.; Uheida, A.; Muhammed, M.; Zou, X.; Dutta, J. Rare Earth Ions Adsorption onto Graphene Oxide Nanosheets. *Solvent Extr. Ion Exch.* **2017**, *35*, 91–103. [CrossRef]
38. Matsunaga, H.; Ismail, A.; Wakui, Y.; Yokoyama, T. Extraction of Rare Earth Elements with 2-Ethylhexyl Hydrogen 2-Ethylhexyl Phosphonate Impregnated Resins Having Different Morphology and Reagent Content. *React. Funct. Polumers* **2001**, *49*, 189–195. [CrossRef]
39. İnan, S.; Tel, H.; Sert, Ş.; Çetinkaya, B.; Sengül, S.; Özkan, B.; Altaş, Y. Extraction and Separation Studies of Rare Earth Elements Using Cyanex 272 Impregnated Amberlite XAD-7 Resin. *Hydrometallurgy* **2018**, *181*, 156–163. [CrossRef]
40. Mondal, S.; Ghar, A.; Satpati, A.K.; Sinharoy, P.; Singh, D.K.; Sharma, J.N.; Sreenivas, T.; Kain, V. Recovery of Rare Earth Elements from Coal Fly Ash Using TEHDGA Impregnated Resin. *Hydrometallurgy* **2019**, *185*, 93–101. [CrossRef]
41. Borra, C.R.; Pontikes, Y.; Binnemans, K.; Van Gerven, T. Leaching of Rare Earths from Bauxite Residue (Red Mud). *Miner. Eng.* **2015**, *76*, 20–27. [CrossRef]
42. Asadollahzadeh, M.; Torkaman, R.; Torab-Mostaedi, M. Extraction and Separation of Rare Earth Elements by Adsorption Approaches: Current Status and Future Trends. *Sep. Purif. Rev.* **2021**, *50*, 417–444. [CrossRef]
43. Singh, I.; Sidana, J.; Bansal, P.; Foley, W. Phloroglucinol Compounds of Therapeutic Interest: Global Patent and Technology Status. *Expert Opin. Ther. Pat.* **2009**, *19*, 847–866. [CrossRef] [PubMed]
44. Abdel-Ghany, S.; Day, I.; Heuberger, A.; Broeckling, C.; Reddy, A. Production of Phloroglucinol, a Platform Chemical, in Arabidopsis Using a Bacterial Gene. *Sci. Rep.* **2016**, *6*, 38483. [CrossRef]
45. Li, X.; Jia, P.; Wang, T. Furfural: A Promising Platform Compound for Sustainable Production of C4 and C5 Chemicals. *ACS Catal.* **2016**, *6*, 7621–7640. [CrossRef]
46. Mattioda, G.; Blanc, A. *Ullmann's Encyclopedia of Industrial Chemistry*; Wiley-VCH: Weinheim, Germany, 2011.
47. Khawassek, Y.M.; Eliwa, A.A.; Haggag, E.S.A.; Omar, S.A.; Abdel-Wahab, S.M. Adsorption of Rare Earth Elements by Strong Acid Cation Exchange Resin Thermodynamics, Characteristics and Kinetics. *SN Appl. Sci.* **2018**, *1*, 51. [CrossRef]
48. Sahoo, T.R.; Prelot, B. Chapter 7—Adsorption Processes for the Removal of Contaminants from Wastewater: The Perspective Role of Nanomaterials and Nanotechnology. In *Nanomaterials for the Detection and Removal of Wastewater Pollutants*; Bonelli, B., Freyria, F.S., Rossetti, I., Sethi, R., Eds.; Elsevier: Amsterdam, The Netherlands, 2020; pp. 161–222.
49. Shu, Z.; Xiong, C.; Shen, Q.; Yao, C.; Gu, Z. Adsorption Behavior and Mechanism of D113 Resin for Lanthanum. *Rare Met.* **2007**, *26*, 601–606. [CrossRef]
50. Zheng, Z.; Xiong, C. Adsorption Behavior of Ytterbium (III) on Gel-Type Weak Acid Resin. *J. Rare Earths* **2011**, *29*, 407–412. [CrossRef]
51. Araucz, K.; Aurich, A.; Kołodyńska, D. Novel Multifunctional Ion Exchangers for Metal Ions Removal in the Presence of Citric Acid. *Chemosphere* **2020**, *251*, 126331. [CrossRef]
52. Bezzina, J.P.; Ogden, M.D.; Moon, E.M.; Soldenhoff, K.L. REE Behavior and Sorption on Weak Acid Resins from Buffered Media. *J. Ind. Eng. Chem.* **2018**, *59*, 440–455. [CrossRef]
53. Fan, Q.; Tan, X.; Li, J.; Wang, X.; Wu, W.; Montavon, G. Sorption of Eu(III) on Attapulgite Studied by Batch, XPS, and EXAFS Techniques. *Environ. Sci. Technol.* **2009**, *43*, 5776–5782. [CrossRef] [PubMed]
54. Saha, P.; Chowdhury, S. Insight Into Adsorption Thermodynamics. In *Thermodynamics*; Mizutani, T., Ed.; IntechOpen: London, UK, 2011. [CrossRef]
55. Judge, W.; Azimi, G. Recent Progress in Impurity Removal during Rare Earth Element Processing: A Review. *Hydrometallurgy* **2020**, *196*, 105435. [CrossRef]
56. Apelblat, A. Dissociation Equilibria in Solutions with Citrate Ions. In *Citric Acid*; Apelblat, A., Ed.; Springer International Publishing: Cham, Switzerland, 2014; pp. 143–212, ISBN 978-3-319-11233-6. [CrossRef]

57. Wang, R.; Zheng, Z. Rare Earth Complexes with Carboxylic Acids, Polyaminopolycarboxylic Acids, and Amino Acids. In *Rare Earth Coordination Chemistry: Fundamentals and Applications*; John Wiley & Sons: Singapore, 2010; pp. 91–136. [CrossRef]
58. Belfqueh, S.; Chapron, S.; Giusti, F.; Pellet-Rostaing, S.; Seron, A.; Menad, N.; Arrachart, G. Selective Recovery of Rare Earth Elements from Acetic Leachate of NdFeB Magnet by Solvent Extraction. *Sep. Purif. Technol.* **2024**, *339*, 126701. [CrossRef]
59. Langmuir, I. The Adsorption of Gases on Plane Surfaces of Glass, Mica and Platinum. *J. Am. Chem. Soc.* **1918**, *40*, 1361–1403. [CrossRef]
60. Ghosal, P.S.; Gupta, A.K. Determination of Thermodynamic Parameters from Langmuir Isotherm Constant-Revisited. *J. Mol. Liq.* **2017**, *225*, 137–146. [CrossRef]
61. Limousin, G.; Gaudet, J.-P.; Charlet, L.; Szenknect, S.; Barthès, V.; Krimissa, M. Sorption Isotherms: A Review on Physical Bases, Modeling and Measurement. *Appl. Geochem.* **2007**, *22*, 249–275. [CrossRef]
62. Freundlich, H. Über Die Adsorption in Lösungen. *Z. für Phys. Chem.* **1907**, *57U*, 385–470. [CrossRef]
63. Azizian, S. Kinetic Models of Sorption: A Theoretical Analysis. *J. Colloid Interface Sci.* **2004**, *276*, 47–52. [CrossRef]
64. Simonin, J.-P. On the Comparison of Pseudo-First Order and Pseudo-Second Order Rate Laws in the Modeling of Adsorption Kinetics. *Chem. Eng. J.* **2016**, *300*, 254–263. [CrossRef]
65. Lagergren, S. Zur Theorie Der Sogenannten Adsorption Geloster Stoffe. *K. Sven. Vetenskapsakademiens. Handl.* **1898**, *24*, 1–39.
66. Ho, Y.S. Citation Review of Lagergren Kinetic Rate Equation on Adsorption Reactions. *Scientometrics* **2004**, *59*, 171–177. [CrossRef]
67. Cheung, C.W.; Porter, J.F.; McKay, G. Sorption Kinetics for the Removal of Copper and Zinc from Effluents Using Bone Char. *Sep. Purif. Technol.* **2000**, *19*, 55–64. [CrossRef]
68. Das, A.; Chandrakumar, K.R.S.; Paul, B.; Chopade, S.M.; Majumdar, S.; Singh, A.K.; Kain, V. Enhanced Adsorption and Separation of Zirconium and Hafnium under Mild Conditions by Phosphoric Acid Based Ligand Functionalized Silica Gels: Insights from Experimental and Theoretical Investigations. *Sep. Purif. Technol.* **2020**, *239*, 116518. [CrossRef]
69. Trieu, Q.A.; Pellet-Rostaing, S.; Arrachart, G.; Traore, Y.; Kimbel, S.; Daniele, S. Interfacial Study of Surface-Modified ZrO_2 Nanoparticles with Thioctic Acid for the Selective Recovery of Palladium and Gold from Electronic Industrial Wastewater. *Sep. Purif. Technol.* **2020**, *237*, 116353. [CrossRef]
70. Ho, Y.S.; McKay, G. Pseudo-Second Order Model for Sorption Processes. *Process Biochem.* **1999**, *34*, 451–465. [CrossRef]
71. Vadivelan, V.; Kumar, K.V. Equilibrium, kinetics, mechanism, and process design for the sorption of methylene blue onto rice husk. *J. Colloid Interface Sci.* **2005**, *286*, 90–100. [CrossRef] [PubMed]
72. Plazinski, W.; Dziuba, J.; Rudzinski, W. Modeling of Sorption Kinetics: The Pseudo-Second Order Equation and the Sorbate Intraparticle Diffusivity. *Adsorption* **2013**, *19*, 1055–1064. [CrossRef]